Small tip angle NMR as a probe of electron-mediated nuclear spin-spin couplings in YBa$_2$Cu$_3$O$_7$

C. H. Pennington,[1] S. Yu,[1] K. R. Gorny,[1] M. J. Buoni,[1] W. L. Hults,[2] and J. L. Smith[2]

[1]*Department of Physics, The Ohio State University, 174 W. 18th Avenue, Columbus, Ohio 43210*
[2]*Los Alamos National Laboratory, Los Alamos, New Mexico 87545*

We develop the theory and application of small tip angle NMR techniques that can be used to measure couplings between nuclear spins and multiple neighboring spins. We employ the techniques to measure indirect (electron-mediated) nuclear spin-spin couplings between neighboring ^{63,65}Cu and ^{17}O nuclear spins in the high-temperature superconductor YBa$_2$Cu$_3$O$_7$. Predictions for the values of these couplings can be obtained from the existing phenomenological models of electronic spin susceptibility $\chi(\mathbf{q},\omega)$ and hyperfine couplings that have been used in attempts to understand the wide body of YBa$_2$Cu$_3$O$_7$ NMR data gathered to date. We find that the measured couplings are incompatible with these models.

I. INTRODUCTION

High-temperature superconductors have been the subject of the most thorough NMR investigations of any solid-state system.[1–3] There is rich and contrasting NMR behavior at all of the eight distinct atomic sites within the unit cell of YBa$_2$Cu$_3$O$_{7-\delta}$, most notably within the CuO$_2$ planes. The most widely known anomaly is that the temperature dependences of the planar ^{17}O and ^{63}Cu spin-lattice relaxation rates $^{17}(T_1T)^{-1}$ and $^{63}(T_1T)^{-1}$ are drastically different, despite the very close proximity ($\sim$1.9 Å) of these atoms within the unit cell. Further obscuring the picture, it is found that the temperature dependences of the ^{17}O and ^{63}Cu Knight shifts are identical to each other. Interpretation of these and other confusing NMR findings have required a detailed picture of the various hyperfine couplings and of electron-spin dynamics. An early consensus[4–7] developed around a coupling of both ^{17}O and ^{63}Cu to the same unpaired electron spins in the Cu $3d(x^2-y^2)$ orbitals. This consensus gave a simple explanation for the identical ^{17}O and ^{63}Cu Knight-shift behaviors. The drastically different behaviors of $^{17}(T_1T)^{-1}$ and $^{63}(T_1T)^{-1}$ resulted, within this model, from electron-spin correlations and "form-factor" effects. For example, ^{17}O is situated halfway between two Cu electron moments, and thus its couplings to its two Cu neighbor electron spins will cancel if the spins are oppositely oriented. In other words, ^{17}O NMR does not couple to fluctuations near the antiferromagnetic wave vector. In contrast ^{63}Cu NMR can be affected by fluctuations at any wave vector. The model then can permit very different ^{17}O and ^{63}Cu NMR behaviors, even though ^{17}O and ^{63}Cu couple to the same system of electrons. Over the years this model has been used to interpret a wide body of NMR data. Within this "one-component model," hyperfine couplings are now tightly constrained by T_1 and Knight-shift experiments.

Despite the successes of the one component model, cases have emerged in which it has clearly failed. First, Walstedt and co-workers[8–10] have shown that a comparison of inelastic neutron-scattering results and NMR lead to the conclusion that the ^{17}O hyperfine coupling to the Cu^{2+} moments is much weaker than required. Second, measurements of

^{17}O T_1 anisotropy[11,12] (dependence on magnetic-field orientation) have revealed a temperature dependence which is unexpected in the simplest one-component formulation, but which has been addressed[13] by postulating that ^{17}O is coupled not only to nearest-neighbor Cu^{2+} moments but also to next-nearest neighbors. Finally, Nandor *et al.*[14] and Takigawa *et al.*[15] have demonstrated anomalies in the behaviors of ^{17}O and ^{89}Y Knight shift and T_1 which are quite inconsistent with a one-component picture, even allowing for the more general ^{17}O hyperfine coupling.

Here we present yet another category of experiment for which the one-component model is inadequate, namely experiments probing electron-mediated couplings between nuclear spins. These couplings result from the real part $\chi'(\mathbf{q},\omega)$ of the electron-spin susceptibility—in the simplest case a nucleus, which we take to be at the origin, hyperfine couples to its on-site electron spin. The electron spin system then responds with a spatial distribution of spin density proportional to $\chi'(\mathbf{r},\omega=0)$. That distribution then interacts with neighboring nuclei, so that they experience an "effective" coupling to the nucleus at the origin.

Most experiments to date that have probed electron mediated nuclear-spin couplings have consisted of measurements of "$T_{2\mathrm{G}}$," the time constant for the approximately Gaussian decay which is observed in measurements of ^{63}Cu spin-echo amplitudes vs 2τ, where τ is the time interval between the 90 and 180° pulses of a spin-echo sequence. $T_{2\mathrm{G}}$ specifies only the sum of the squares of the couplings of a nuclear spin to its neighbors, but not the coupling to individual neighbors. In this sense $T_{2\mathrm{G}}$ is a crude measurement, yet its utility has been widely recognized and exploited.[16–33]

More recently our group[34–36] has demonstrated interesting experimental techniques, "small tip angle NMR," which have made it possible to go beyond $T_{2\mathrm{G}}$ and to measure individual electron-mediated couplings between nuclear spins. Specifically, Gorny *et al.*[34] and Yu *et al.*[36] measured respectively the nearest-neighbor ^{63}Cu-^{63}Cu and ^{63}Cu-^{17}O coupling strengths in YBa$_2$Cu$_3$O$_7$ and discussed implications for the one component model. Intuitively one expects these couplings, $^{63,63}a$ and $^{63,17}a$, to be quite sensitive to the electron-spin correlations which result in the very different

behaviors of $^{63}(T_1T)^{-1}$ and $^{17}(T_1T)^{-1}$. The form-factor effects which are thought to shield the antiferromagnetic fluctuations from the ^{17}O should also reduce the electron mediated coupling $^{63,17}a$ between ^{63}Cu and ^{17}O, relative to the ^{63}Cu-^{63}Cu coupling, $^{63,63}a$. Yu *et al.*, however, found that this expectation was not met.

In this paper we present and demonstrate more fully the experimental methodologies employed by Gorny *et al.* and Yu *et al.* We develop the theory of small tip angle NMR and demonstrate its application on a model system. We provide further experimental confirmation of the key results of Gorny *et al.* and Yu *et al.* through double-resonance NMR techniques, forbidden transition spectroscopy, isotope dependence tests, pulse flipping effectiveness measurements, tests for mutual spin flips, and measurements at new temperature and dopant ranges. We re-emphasize and elaborate upon the incompatibility with one-component models used in analysis of previous NMR data, and suggest directions for new attacks upon the problem.

In Sec. II we introduce the small tip angle NMR techniques and demonstrate their application on a model system. In Sec. III we apply these and other techniques to the measurement of indirect couplings in high-T_c cuprates. Finally in Sec. IV we discuss implications.

II. SMALL TIP ANGLE NMR

Now we describe and demonstrate the small tip angle NMR techniques that we have developed specifically for the problem of measuring indirect couplings in high-T_c superconductors.

NMR, as used to extract internuclear couplings, including direct magnetic dipolar couplings as well as "indirect," electron-mediated couplings,[37,38] has long been a valuable source of structural information about both solid and liquids.[39,40] Often, however, the couplings result in broad and/or complex NMR line shapes which can only be treated using unsatisfactory approximations. One fundamental reason for this difficulty is that the splittings resulting from couplings with the various individual neighbors are not observed in isolation, but rather they are all present at once, and their effects are mutually convoluted. As an example, the spectrum for a proton in solution which has scalar J couplings to N inequivalent spin-$\frac{1}{2}$ neighbors will display 2^N distinct peaks at frequencies which are sums and differences of the N coupling frequencies, while only N peaks would result were the multiple couplings to remain unconvoluted. For the case of liquid state NMR, only the scalar couplings between spins within the same molecule are effective, and so N is often small enough that it is possible to "deconvolute" and infer the various couplings. However for the case of solids N is often too large. In $YBa_2Cu_3O_7$ for example the prevalent analysis[5,25] of T_1 and shift measurements lead one to expect a long antiferromagnetic correlation length that results in a ^{63}Cu nucleus having couplings to 20–30 or more neighbors. To measure these couplings individually it is necessary to avoid the complexity of the large number of peaks ($\sim 2^{20-30}$) that are expected.

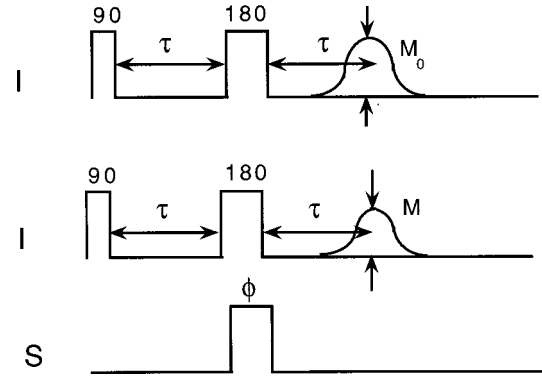Here we present a theoretical description and experimen-

FIG. 1. The small tip angle double-resonance (STIPDOR) sequence, shown above, is a generalized version of the spin-echo double-resonance (SEDOR) sequence. The spin-echo sequence is applied to spin I (observed), both with and without an accompanying ϕ pulse applied to the S spin system. While in SEDOR ϕ is equal to π, in the STIPDOR sequence the angle ϕ is $\ll 1$.

tal realization of a double-resonance pulse sequence, small tip angle double resonance (STIPDOR), which is a generalization of the spin-echo double-resonance (SEDOR) sequence,[24,41,42] but which, in contrast to the usual SEDOR experiment, results in a spectrum containing directly the unconvoluted distribution of heteronuclear coupling frequencies. This technique has since been incorporated into rotational echo double-resonance (REDOR) NMR measurements of bond lengths.[35,43] In addition we present a theoretical description of an analogous single-resonance sequence to measure homonuclear couplings, small tip angle echo resonance (STAGGER).

A. Double-resonance STIPDOR techniques

The double-resonance STIPDOR and related SEDOR techniques are used to measure spin couplings between "unlike" nuclei which have resonances at clearly distinct frequencies. For example, in a 10-T field ^{63}Cu resonates at ~ 113 MHz, while ^{17}O is at ~ 58 MHz. One can easily monitor and manipulate these two resonances separately. We consider a large static field applied parallel to the z axis. Then we consider a nuclear spin I, under observation, coupled to N "unlike" spins S_n ($n=1\cdots N$) in the following way (all spins taken to be $\frac{1}{2}$):

$$H/\hbar = \sum_{n=1}^{N} a_n I_z S_{nz}. \quad (1)$$

This Hamiltonian is appropriate in many situations of interest—for example, for heteronuclear J coupling the values a_n are equal to corresponding J_n's, while for heteronuclear dipole coupling a_n is given by the well-known expression $a_n = (\gamma_I \gamma_S \hbar / r^3)(1 - 3\cos^2\theta)$. The Hamiltonian [Eq. (1)] is also that which is assumed in the analysis of the spin-echo double-resonance (SEDOR) experiments. For example, in this paper we perform double-resonance experiments in which the I spin, ^{17}O, is coupled to S spins, ^{63}Cu. The standard SEDOR sequence is illustrated in Fig. 1.

SEDOR is a two part experiment: in part one, a conventional spin-echo sequence is applied to the I spins, with a spacing τ between the $\pi/2$ and π pulses. The amplitude M_0 of the I spin echo at time $t = 2\tau$ is then recorded. Subsequently, the I spin echo is repeated; however, coincident with the application of the π pulse to the I spins, an additional pulse of flip angle ϕ (equal to π in conventional SEDOR) is applied to the S spins. The amplitude M of the I spin echo for this second echo is then recorded. The SEDOR signal, defined as $m = M/M_0$, can then be obtained, and its dependence $m(t)$ on the time t provides a certain measure of internuclear coupling effects, distilled from effects unrelated to the internuclear couplings. In particular, if the angle ϕ is equal to π, the SEDOR signal $m(t)$ is given as

$$m(t) = \prod_{n=1}^{N} \cos(a_n t). \qquad (2)$$

Thus in the SEDOR signal the sinusoidal time dependences which would result from each coupling element a_n individually will appear as products. In the Fourier domain these couplings will be convoluted, resulting in 2^N peaks occurring at frequency values given by $\pm a_1/2 \pm a_2/2 \pm a_3/2 \cdots \pm a_N/2$. In the STIPDOR sequence we relax the condition that ϕ, the nutation angle for flipping the S spins in SEDOR, is equal to π. In particular, we will examine the case of $\phi \ll \pi$. The utility of using values of ϕ not equal to π in the SEDOR experiment was first emphasized by Cull et al.,[44] who demonstrated that, by measuring the dependence m on ϕ for a a single large value of t, one could extract the number of S neighbors. In contrast, in the STIPDOR experiment we examine, for a single, small value of ϕ, the dependence of m upon t. Classically, this limit will represent the case where very few of the neighboring S spins are flipped—in fact we shall consider the limit where the probability is negligible that more than one neighboring S spin is flipped. STIPDOR will yield not only the number of S spin neighbors but also the coupling J_n of each. For a general flip angle ϕ, the expression for the SEDOR signal $m(t)$ becomes

$$m(t) = \prod_{n=1}^{N} \left[\cos^2(\phi/2) + \sin^2(\phi/2)\cos(a_n t/2)\right]. \qquad (3)$$

The term $\sin^2(\phi/2)$ here has a simple physical interpretation—namely, it is the probability that pulse of tip angle ϕ will flip a given spin. [$\cos^2(\phi/2)$ is, of course, the probability that a neighbor will *not* be flipped.] For small ϕ we expand the cosine and sine terms to obtain

$$m(t) \approx \prod_{n=1}^{N} \left\{[1-(\phi/2)^2] + (\phi/2)^2 \cos(a_n t/2)\right\}. \qquad (4)$$

Including only terms up to order $(\phi/2)^2$ we find that the product reduces to a sum

$$m(t) \approx [1 - N(\phi/2)^2] + (\phi/2)^2 \sum_{n=1}^{N} \cos(a_n t/2). \qquad (5)$$
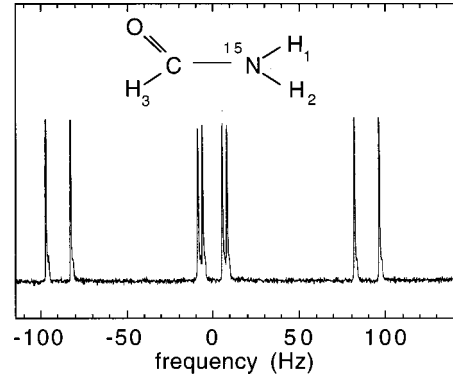

FIG. 2. ^{15}N NMR line shape of formamide. Line shape is obtained by Fourier transform of the free induction decay (FID) signal. Formamide molecule is also illustrated. The ^{15}N nucleus is coupled to three inequivalent protons, labeled H_1, H_2, and H_3. Protons H_1 and H_2 are rendered inequivalent due to the partial double bond character of the N-C bond. Line shape shows the eight expected peaks at frequencies $(\frac{1}{2})[\pm J_1 \pm J_2 \pm J_3]$ (equal to ± 96.3, ± 89, ± 8.4, and ± 5.8 Hz, with $J_1 = 90.5$ Hz, $J_2 = 87.8$ Hz, and $J_3 = 14.2$ Hz, respectively).

The condition of validity for this final approximation is that quantity $N(\phi/2)^2$ must be small compared to one, or equivalently that the fractional destruction of the I spin echo which results from application of the ϕ pulse to the S spins is small. We may also describe the condition for validity as follows: in order for Eq. (5) to be valid, there must be a negligible probability that *more than one* neighbor is flipped. One may Fourier transform $m(t)$ to obtain

$$m(\omega) \approx [1 - N(\phi/2)^2]\delta(\omega) + \tfrac{1}{2}(\phi/2)^2$$
$$\times \sum_{n=1}^{N} [\delta(\omega - a_n/2) + \delta(\omega + a_n/2)]. \qquad (6)$$

The remarkable feature of Eq. (6) is that the time dependence of $m(t)$ contains only the coupling frequencies $a_n/2$, rather than the sum and difference frequencies $\pm a_1/2 \pm a_2/2 \pm a_3/2 \cdots \pm a_N/2$ which appear in the free induction decay and in conventional SEDOR. We demonstrate the STIPDOR method using ^{15}N labeled formamide, a liquid with molecular structure shown in Fig. 2. ^{15}N experiences J coupling to each of the three inequivalent protons, with coupling values J_1, J_2, and J_3 given by 90.5, 87.8, and 14.2 Hz, respectively. Figure 2 gives the ^{15}N NMR line shape, obtained on a conventional high-resolution NMR spectrometer, by Fourier transform of the free induction decay signal. As expected, eight, or 2^3, peaks appear at frequencies $(\frac{1}{2})[\pm J_1 \pm J_2 \pm J_3] = \pm 96.2$, ± 82.0, ± 8.4, and ± 5.8 Hz. Figure 3 gives, for comparison, ^{15}N line shapes (positive frequencies only) obtained by STIPDOR (the sequence illustrated in Fig. 1), with $I = {}^{15}$N and $S = {}^{1}$H. The STIPDOR signal $m(t)$ (defined above) is taken as a function of t, which is twice the spacing between the 90 and 180° pulses. $m(t)$ is then Fourier transformed. The results, along with theoretical predictions, are given in Fig. 3 for pulse angles $\phi = 30°$, 90°, and 180°. The probabilities of flipping 0, 1, 2, and 3 neigh-
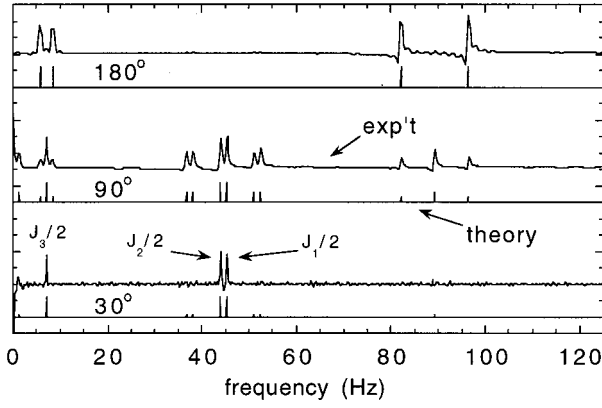
FIG. 3. Experimental and theoretical ^{15}N small tip angle double-resonance (STIPDOR, as in Fig. 1) NMR line shapes of formamide, using tip angles ϕ (as defined in Fig. 1) of $\phi = 30°$, $90°$, and $180°$. The line shapes are obtained by Fourier transform of the echo height ratio M/M_O (as defined in Fig. 1) with respect to 2τ, where τ is the pulse spacing as in Fig. 1. The line shape for $\phi = 180°$ (conventional SEDOR) reproduces the conventional free induction decay (FID) NMR line shape of Fig. 2, as expected, with peaks at $|(\frac{1}{2})[\pm J_1 \pm J_2 \pm J_3]| =$ to 96.3, 89, 8.4, and 5.8 Hz. (Only positive frequencies are shown.) In contrast the $\phi = 30°$ STIPDOR line shapes has features only at $J_1/2$, $J_2/2$, and $J_3/2$, equal to 45.2, 43.9, and 7.1 Hz. The intermediate case, $\phi = 90°$, contains 13 peaks, enumerated in the text.

bors are given by successive terms in the expansion $[\cos^2(\phi/2) + \sin^2(\phi/2)]^3$; equal to 0.81, 0.17, 0.013, and 3×10^{-4}. Thus in the $\phi = 30°$ line shape one may neglect the probabilities that two or more neighbors will be flipped. In this limit STIPDOR gives the coupling frequencies $J_1/2$, $J_2/2$, and $J_3/2$ directly. These features are seen clearly in Fig. 3 at the expected values of 45.2, 43.9, and 7.1 Hz. Absent in the line shape are features at the frequencies $|(\frac{1}{2})[\pm J_1 \pm J_2 \pm J_3]|$ (equal to 96.2, 82.0, 8.4, and 5.8 Hz) which are observed in the free induction decay (Fig. 2) and which would be observed in conventional SEDOR. Also absent are the features at $|(\frac{1}{2})[\pm J_1 \pm J_2]|$, $|(\frac{1}{2})[\pm J_1 \pm J_3]|$, and $|(\frac{1}{2})[\pm J_2 \pm J_3]|$ (equal to 89.1, 1.3, 52.3, 38.1, 51.0, and 36.8 Hz). These frequencies correspond to flipping two neighboring spins—an improbable event for a 30° pulse. The STIPDOR line shape for $\phi = 90°$ is predicted and observed to be much more rich, because for $\phi = 90°$ the probabilities of flipping 0, 1, 2, and 3 neighbors are all non-negligible. The $\phi = 90°$ STIPDOR line shape, along with the theoretical prediction, clearly displays each of the 13 (positive) frequencies enumerated above, with the expected intensities.

STIPDOR for $\phi = 180°$ reduces to conventional SEDOR. The experimental result of Fig. 3 shows clearly peaks at frequencies $|(\frac{1}{2})[\pm J_1 \pm J_2 \pm J_3]|$, the same peaks which are observed in the free induction decay of Fig. 2. The remarkable fulfillment of predictions shown in Fig. 3 demonstrates that the simple way of thinking outlined above, in terms of spin flip probabilities, is appropriate and correct.
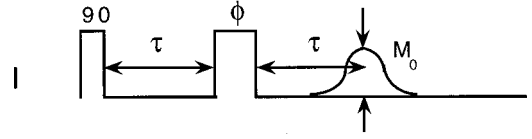

FIG. 4. The small tip angle echo resonance (STAGGER) sequence.

B. Single-resonance STAGGER technique for homonuclear couplings

Now we briefly describe a technique which extends the principle of STIPDOR to probe *homonuclear* couplings, small tip angle echo resonance (STAGGER). In Sec. III we use this technique to probe homonuclear ^{63}Cu-^{63}Cu couplings. Here we suppose that the I spin nucleus is coupled to N other spins which are of the same nuclear species, but which are inequivalent in the sense that they are chemically shifted from one another by an amount exceeding their internuclear couplings. (These assumptions are valid for ^{63}Cu in YBa$_2$Cu$_3$O$_7$, with the applied field parallel to c, as discussed in Refs. 24, 25, and 45.) We take, for the case of an applied field parallel to the z axis, the following spin coupling Hamiltonian:

$$H/\hbar = \sum_{n=1}^{N} a_n I_z I_{nz}. \qquad (7)$$

Figure 4 illustrates the simple STAGGER sequence. First the sequence 90-τ-ϕ-τ-echo is applied, and the resulting echo amplitude $M(t=2\tau)$ will be given by

$$M(t) = \sin^2(\phi/2) \prod_{n=1}^{N} \left[\cos^2(\phi/2) + \sin^2(\phi/2)\cos(a_n t/2)\right] h(t). \qquad (8)$$

The function $h(t)$ is the decay that results from factors other than homonuclear coupling, and we ignore it for the moment. The prefactor $\sin^2(\phi/2)$ reflects only the expected drop in echo size when ϕ is less than $180°$. The terms $\sin^2(\phi/2)$ and $\cos^2(\phi/2)$ appearing in the product, however, have the same interpretation as in Eq. (5): $\sin^2(\phi/2)$ is the probability that any given neighboring spin will be flipped (by $\Delta m = \pm 1$) by the pulse of angle ϕ, while $\cos^2(\phi/2)$ is the probability that it will not be flipped. For the case of *small tip angle* ($\phi \ll 1$), Eq. (8) reduces to [suppressing $h(t)$]

$$M(t) \approx (\phi/2)^2 \left([1 - N(\phi/2)^2] + (\phi/2)^2 \sum_{n=1}^{N} \cos(a_n t/2) \right). \qquad (9)$$

Equation (9) shows that, like STIPDOR, the STAGGER sequence also yields the unconvoluted distribution of couplings. STAGGER, however, is a single resonance method for measurement of homonuclear couplings.

Now we comment briefly on $h(t)$ in the STAGGER sequence. In general one may control for $h(t)$ by first running STAGGER with a tip angle ϕ, then again with angle 2ϕ. By taking the ratio of the signal obtained in the 2ϕ case to that
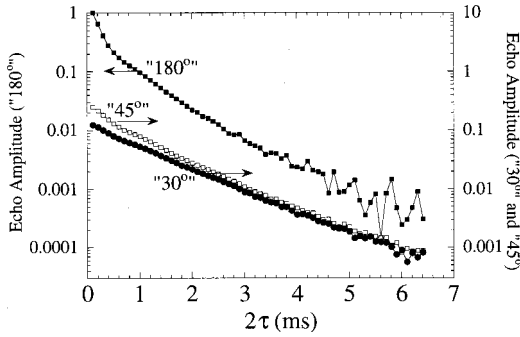
FIG. 5. ^{63}Cu(2) echo amplitude (for planar Cu in YBa$_2$Cu$_3$O$_7$) vs 2τ, at $T=5$ K with a field of 9 T along the c axis of the aligned powder sample, for the STAGGER NMR pulse sequence ''90-τ-ϕ-τ-echo.'' Results for $\phi=$''30,'' ''45,'' and ''180'' are shown.

obtained for ϕ one may cancel the unknown $h(t)$. This procedure however requires a very high signal to noise ratio. For the case of our high-T_c experiments (reported in Sec. III) we artificially remove what we think to be $h(t)$ and compare results for several values of ϕ.

III. EXPERIMENT: MEASUREMENTS OF ELECTRON-MEDIATED NUCLEARSPIN-SPIN COUPLINGS IN YBa$_2$Cu$_3$O$_7$

We now turn to the application of small tip angle NMR to YBa$_2$Cu$_3$O$_7$. In Secs. III A and B we describe the array of experiments which measure the nearest-neighbor ^{63}Cu-^{63}Cu coupling $(2\pi)^{-1}[^{63,63}a/2]=(900\pm100)$ Hz and ^{17}O-^{63}Cu coupling $(2\pi)^{-1}[^{17,63}a/2]=(147\pm10)$ Hz. In Sec. III C we describe the mathematical connection between these couplings and the parameters used in previous one-component models, and the severe conflict that these measurements present.

A. ^{63}Cu-^{63}Cu couplings

One expects[24,25,36,45] for the case of ^{63}Cu NMR in YBa$_2$Cu$_3$O$_7$, with magnetic field applied parallel to c, that the Hamiltonian of Eq. (7) is an adequate description of the effects of ^{63}Cu-^{63}Cu spin-spin coupling. Here we focus on experimental results establishing the value for the nearest-neighbor ^{63}Cu-^{63}Cu coupling $(2\pi)^{-1}[^{63,63}a/2]=(900\pm100)$ Hz.

Figure 5 contains results of application of STAGGER on the ^{63}Cu(2) in YBa$_2$Cu$_3$O$_7$, at a field of 9 T along the aligned powder c axis, and with $T=5$ K, as reported in our previous work.[34] Shown are results for $\phi=$''30°,'' ''45°,'' and ''180°.'' Quotation marks denote that in the superconducting state the rf fields used to apply pulses are screened by supercurrents, so that what is for example a 180° pulse near the surface of the sample may be a much smaller angle pulse as one moves deeper into the sample. The ''180°'' pulse maximized the echo size, and the ''30°'' and ''45°'' pulses were of $\frac{1}{6}$ and $\frac{1}{4}$ the time duration of the ''180°'' pulse.
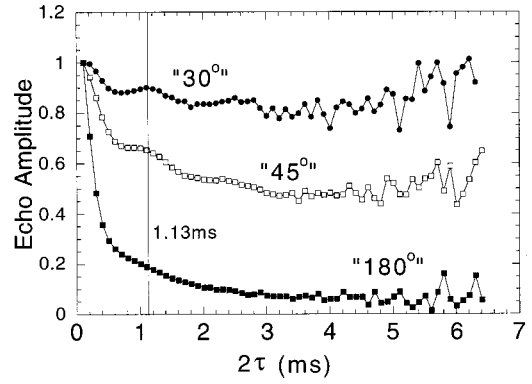

FIG. 6. Data of Fig. 5, but multiplied by a factor $\exp(2\tau/1.209$ ms$)$, removing the observed exponential decay.

The results for all three angles ϕ exhibit an overall exponential decay (though modulated, as we shall see), with time constant 1.209 ms. For now, we take this exponential decay to be the ''$h(t)$'' appearing in Eq. (8), the decay resulting from causes other than homonuclear ^{63}Cu-^{63}Cu coupling. Figure 6 shows the data of Fig. 5 corrected for this $h(t)$. Subsequently we will demonstrate using double resonance that this ''correction'' procedure is valid.

As expected these ''corrected'' data of Fig. 6 display, for the case of ''180°,'' a relatively featureless monotonic decay, as in a conventional ''T_{2G}'' measurement (though we shall subsequently discuss the behavior in more detail). However, for the ''small tip angle'' cases of ''30°'' and ''45°,'' a pronounced sinusoidal modulation, with a period of approximately 1.1 ms is present. (A vertical line at 1.13 ms is given for reference in Fig. 2). The clear meaning of this modulation, with reference to Eq. (5), is that it reveals a ^{63}Cu-^{63}Cu spin-spin coupling frequency of 1.1 ms$^{-1}\approx900\pm100$ Hz.

Since the publication of Ref. 34 we have performed two additional experiments to confirm the coupling frequency $(2\pi)^{-1}[^{63,63}a/2]=(900\pm100)$ Hz. They are a ^{63}Cu-^{65}Cu isotope comparison experiment, and a ^{63}Cu-^{65}Cu double resonance experiment in which we excite a forbidden ^{63}Cu $\Delta m=2$ transition for improved accuracy.

1. ^{63}Cu-^{65}Cu STAGGER isotope comparison

Figure 7 provides a straightforward check of the results of Fig. 6. We applied the STAGGER measurement of Fig. 6 to the ^{65}Cu isotope, which has a gyromagnetic ratio and NMR resonance frequency some 7.1% higher than does ^{63}Cu. ^{65}Cu has a natural abundance of 31%, and ^{63}Cu 69%, so both are highly abundant. This measurement, then, probes the nearest-neighbor coupling between ^{65}Cu's, which is expected to be some 14.8% higher, in the ratio of $(^{65}\gamma/^{63}\gamma)^2$.

As expected, the period of the ^{65}Cu beats of Fig. 7 is found to be substantially shorter than that of ^{63}Cu. We estimate from the data of Fig. 7 that the ^{65}Cu beat frequency is some $(23\pm9)\%$ greater than that of ^{63}Cu, barely within experimental error of 14.8%. The presence of this isotope effect provides some confirmation that the beats seen in the STAGGER experiment do indeed reflect spin-spin coupling.
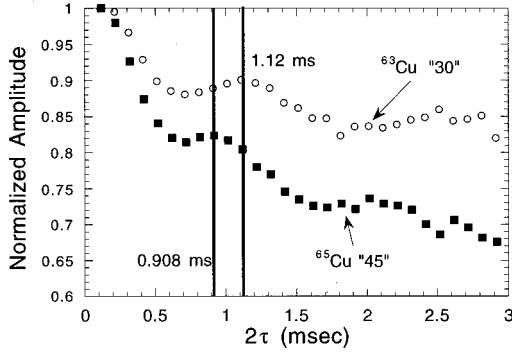
FIG. 7. Open circles are the ^{63}Cu data of Fig. 6, with tip angle 30°. Closed squares are analogous data on ^{65}Cu, with tip angle 45°. Vertical lines are drawn to indicate the approximate period of the prominent beat for each isotope. The lines are drawn at 0.91 ms (^{65}Cu) and at 1.12 ms (^{63}Cu), each with uncertainty estimated at 10%. The ratio $(1.12/0.91)=1.23\pm0.09$ can be compared with the expected value $(^{65}\gamma/^{63}\gamma)^2=1.147$.

In Sec. 2, below, we provide a more convincing demonstration.

2. Confirmation of results using double resonance with forbidden transition

Even with the isotope effect confirmation of Fig. 7, we felt it necessary to further confirm that the beats of Figs. 6 and 7 reflect Cu-Cu spin-spin couplings. The most sure confirmation would be to perform a ^{65}Cu-^{63}Cu SEDOR or STIPDOR measurement (Fig. 1). In such a measurement one would observe the ^{65}Cu echo with and without a flip pulse applied to ^{63}Cu, and then take the ratio of these two echoes to isolate effects on the ^{65}Cu signal resulting solely from the ^{63}Cu flip pulse.

It proved quite difficult to achieve adequate signal to noise with this kind of double-resonance experiment. Furthermore, we noticed that when the experiment was performed in the superconducting state, we found that the ''flip'' pulse had some effect on the ^{65}Cu echo signal even when the flip pulse frequency was set far from the ^{63}Cu NMR intensity. This suggested that perhaps the flip pulse was inducing supercurrents and/or motion of the vortex lattice which persisted even after the pulse ended. There is a possibility that such vortex motion or induced supercurrents could have affected the single-resonance measurements of Fig. 6 as well, and thus we were quite concerned.

It was not possible to perform conventional double resonance (SEDOR or STIPDOR) in the normal state, because the very fast ^{63}Cu T_1's that exist in the normal state also result in rapid Redfield T_2 decays.[24,40] As a result, measurements spanning the full beat period of spin-spin coupling (on the order of 1 ms) proved impractical.

In order to defeat the rapid Redfield T_2 decay we devised a scheme to effectively enhance the spin-spin coupling effect. It was not adequate to observe ^{65}Cu while flipping a conventional $\Delta m=1$ transition of ^{63}Cu. However, a flip of $\Delta m=2$ would double the observed beat frequency and make the measurement practical. Transitions $\Delta m\neq1$ are typically
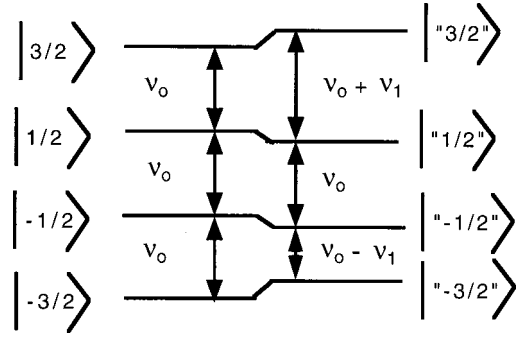

FIG. 8. Energy level diagram for spin-$\frac{3}{2}$ ^{63,65}Cu in the presence of an applied field along z and a quadrupole Hamiltonian, considered as a first-order perturbation. The applied field results in the Zeeman Hamiltonian for which $|m_z=3/2\rangle$, $|1/2\rangle$, $|-1/2\rangle$, and $|-3/2\rangle$ are eigenstates. The quadrupole Hamiltonian gives energy shifts as shown. The final eigenstates are no longer pure eigenstates of the Zeeman Hamiltonian. We label the new states as $|''3/2''\rangle$, $|''1/2''\rangle$, $|''-1/2''\rangle$, and $|''-3/2''\rangle$, as shown.

''forbidden'' in NMR, as the applied radio frequency pulses yield a Hamiltonian $I^{\pm}$ which only connects states separated by $\Delta m=\pm1$. For spin-$\frac{3}{2}$ ^{63}Cu (or ^{65}Cu), however, the presence of an electric-field gradient interaction with the nuclear electric quadrupole moment[40] can allow ''forbidden'' transitions.

The electric quadrupole interaction then adds another term to the Zeeman Hamiltonian H as follows:[2]

$$H/\hbar = -^{63}\gamma B_0(1+K_{zz})I_z+(\omega_Q/2)[I_c^2-I(I+1)/3],\tag{10}$$

where $\mathbf{I}$ is the ^{63}Cu nuclear spin, z is the axis of the applied field, c is the crystal c axis of YBa$_2$Cu$_3$O$_7$, and $\omega_Q/2\pi$ is the nuclear quadrupole resonance frequency of 31.5 MHz. (K is the Knight-shift tensor, which is small compared to the quadrupole Hamiltonian.) Treating the quadrupole term as a perturbation, one obtains, to first order, the schematic energy-level diagram of Fig. 8. The Zeeman levels ($|m_z=3/2\rangle$, $|1/2\rangle$, $|-1/2\rangle$, and $|-3/2\rangle$) find their energy levels shifted. We desire to make our measurement with field parallel to the crystal c axis, in order to reproduce the conditions of the original STAGGER experiments (Figs. 5–7). However, for an applied field parallel to c, the eigenstates of the Hamiltonian are unchanged from the Zeeman eigenstates. Thus in order to ''mix'' the states it was necessary to ''tilt'' the sample with respect to the applied field. We chose a tilt angle of 20° in order to achieve adequate mixing while maintaining an orientation as close as possible to c.

Figure 9 shows the perturbed energy-level splittings and transition matrix elements for ^{65}Cu and ^{63}Cu, for a field of 6 T applied at a 20° angle to the c axis, all obtained by numerical diagonalization of the Hamiltonian. The perturbed states are labeled $|''3/2''\rangle$, $|''1/2''\rangle$, $|''-1/2''\rangle$, and $|''-3/2''\rangle$. For ^{63}Cu we calculate that the $|''1/2''\rangle$ to $|''-3/2''\rangle$ transition will appear at a frequency of ~112 MHz, with a matrix element approximately 19% as large as that for the allowed central transition.
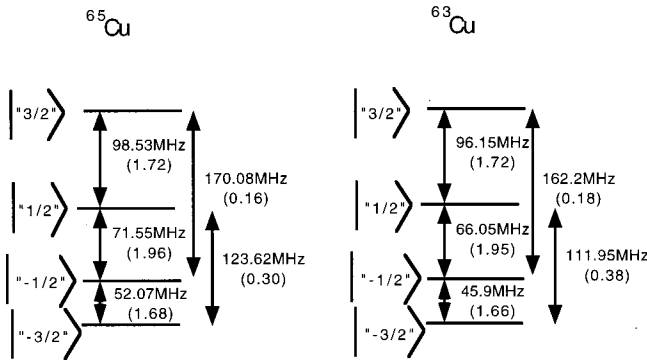
FIG. 9. ^{63}Cu(2) and ^{65}Cu(2) energy-level diagrams with transition frequencies and transition matrix elements, for a 6 T magnetic field applied at a 20° angle to the crystal c axis of YBa$_2$Cu$_3$O$_7$. Magnitudes of transition matrix elements are given in parentheses, directly beneath the frequency for each transition. The ordinarily forbidden $\Delta m = 2$ transition from $|$"1/2"$\rangle$ to $|$"-3/2"$\rangle$ is found to have a matrix element of ~0.38, comparable to (but of course smaller than) those of the allowed $\Delta m = 1$ transitions.

Figure 10 shows the measured line shape, at 100 K, for this forbidden transition, appearing near the expected frequency of 112 MHz. We performed nutation curve measurements on this and other forbidden transitions, and on allowed transitions, and confirmed that the transition matrix elements were close to the expected values. In Fig. 11 we also show transverse relaxation measurements for the allowed ^{65}Cu central transition (T_2 measured as ~85 μs) and the forbidden transition (~40 μs). We can predict an exponential contribution to the transverse decay from Redfield theory[24,40] and known T_1's. This yields Redfield T_2's of 177 μs (central) and 86 μs (forbidden). The faster decays observed in Fig. 11 suggests that spin-spin coupling affects the decay along with the Redfield contribution.

Convinced now that we understand the forbidden transition, we proceed to apply the SEDOR/STIPDOR sequence as shown in Fig. 12, observing a ^{65}Cu allowed transition with and without a flip pulse applied to ^{63}Cu. We performed this experiment at 6 T, and at temperatures 80 and 100 K, obtaining similar results. The results for $T = 80$ K are shown in Fig. 13.
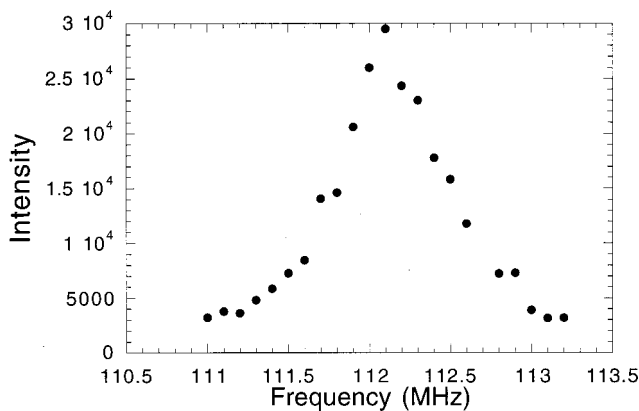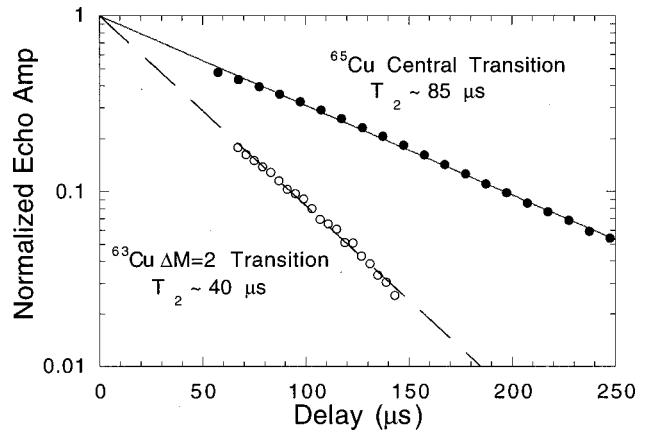

FIG. 11. Echo signal amplitude vs 2τ (where τ is the spacing between 90 and 180° pulses in the spin-echo sequence) for the ^{65}Cu central transition at 71.40 MHz and for the ^{63}Cu $\Delta m = 2$ "forbidden" transition ($\frac{1}{2}$ to $-\frac{3}{2}$) at 112.1 MHz, at temperature 100 K and applied field 6 T. Fits to an exponential yield decay times as indicated in the figure, 85 μs for the ^{65}Cu central transition, and 40 μs for the ^{63}Cu forbidden transition. (The functional forms are not necessarily exponential, though they appear so in within this limit time window.) The Redfield T_2's are expected to be 177 μs (central) and 86 μs (forbidden). The faster rates observed most likely reflect spin-spin coupling effects.

Because we are flipping a $\Delta m = 2$ transition, one expects to observe a beat frequency of approximately twice the frequency observed in Fig. 6; however, one expects an additional 7% boost because we are observing $^{63,65}a$ rather than $^{63,63}a$. The period observed in Fig. 13 is ~0.5 ms, corresponding to a frequency of $\approx (2000 \pm 200)$ Hz. This corresponds to $(2\pi)^{-1}[^{63,63}a/2] = (930 \pm 100)$ Hz, in excellent agreement with the measurement of Fig. 6, $(2\pi)^{-1}[^{63,63}a/2] = (900 \pm 100)$ Hz.

3. Summary of ^{63}Cu-^{63}Cu spin couplings

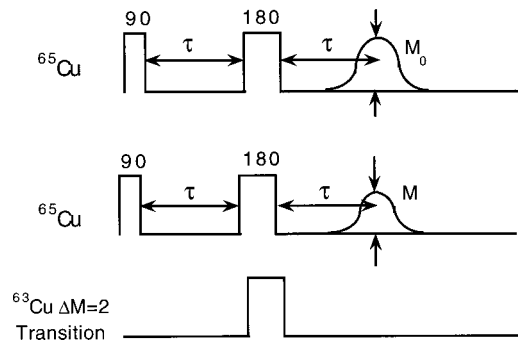Thus not only the single-resonance STAGGER measurement of Fig. 6 and Ref. 34, but also the isotope comparison

FIG. 10. Line shape of the measured $\Delta m = 2$ "forbidden" ^{63}Cu transition, at an applied field of 6 T.

FIG. 12. The SEDOR sequence, applied to ^{65}Cu with and without a flip pulse applied to the ^{63}Cu forbidden transition, with $\Delta m = 2$. The "SEDOR signal" is the ratio M/M_0, and is plotted vs 2τ in Fig. 13 in order to extract information about ^{65,63}Cu spin-spin coupling. The coupling effect though is magnified by a factor of 2 through the application of the $\Delta m = 2$ flip pulse.
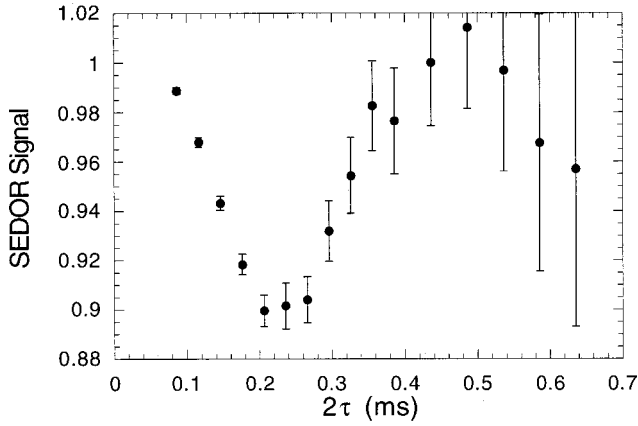
FIG. 13. The forbidden $\Delta m = 2$ transition SEDOR signal (as defined in Fig. 12) M/M_0 vs 2τ, taken at a temperature of 80 K. The beat frequency observed is equal, within experimental error, to twice the beat frequency observed in Fig. 5, which involves the usual $\Delta m = 1$ transition.

and the forbidden transition-based SEDOR experiments confirm the nearest-neighbor ^{63}Cu-^{63}Cu coupling of $(2\pi)^{-1}[^{63,63}a/2] = (900 \pm 100)$ Hz.

B. ^{63}Cu-^{17}O couplings

Having measured the ^{63}Cu-^{63}Cu coupling $^{63,63}a$ we now turn to the measurement of ^{63}Cu-^{17}O coupling, $^{63,17}a$ as originally reported in Ref. 36.

1. Extracting $^{63,17}a$

Our measurements were performed at $T = 4.2$ K on aligned powder samples of $YBa_2Cu_3O_{7-\delta}$ ($T_c = 93$ K), enriched in ^{17}O as in Ref. 46. The applied field of 8 T was oriented parallel to the c axis of the aligned powder. Though the measurements are taken in the superconducting state, one expects on both experimental[22,26,28] and theoretical[17,33] grounds that the quantities measured will take on similar values in the normal state.

The spin-spin coupling effects that are observed between the ^{17}O spin ^{17}I and the ^{63}Cu spin ^{63}I are the result of terms in the effective Hamiltonian

$$H = \sum_{i,j} {}^{63,17}a_{i,j} \, {}^{17}I_{i,z} \, {}^{63}I_{j,z}. \tag{11}$$

Here the sum over i and j are taken over all ^{17}O and ^{63}Cu spins, respectively, and z is the axis of the applied field, the crystal c axis. To measure the ^{17}O-^{63}Cu coupling constant $^{63,17}a$ we employ the STIPDOR generalization of SEDOR described in Sec. II A. In part one, a conventional spin-echo sequence is applied to the ^{17}O spins, with a spacing τ between the $\pi/2$ and π pulses. The amplitude M_0 of the ^{17}O spin echo at time $t = 2\tau$ is then recorded. Subsequently, the spin-echo sequence is repeated; however, coincident with the application of the π pulse to ^{17}O, an additional pulse of flip angle ϕ (equal to π in conventional SEDOR) is applied to
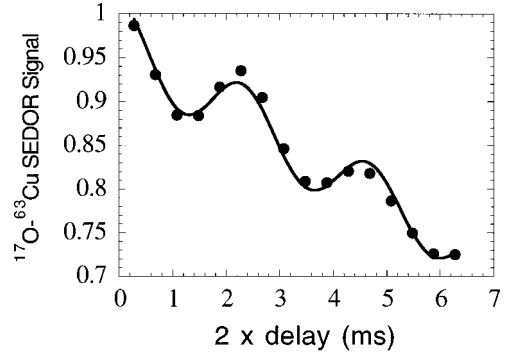

FIG. 14. ^{17}O-^{63}Cu spin-echo double-resonance (SEDOR) signal, observing ^{17}O and flipping ^{63}Cu, vs twice the delay between the ^{17}O 90 and 180° pulses. Temperature is 5 K. Theoretical curve fit, described in the text [Eq. (2)], yields a ^{17}O-^{63}Cu spin-spin coupling frequency $^{17,63}a_{tot}$ of $\frac{1}{2}[^{17,63}a_{tot}/2\pi] = (427 \pm 10)$ Hz.

the ^{63}Cu resonance. The amplitude M of the ^{17}O spin echo for this second echo is then recorded. The SEDOR signal, defined as $m = M/M_0$, can then be obtained, and its dependence $m(t)$ on the time $t = 2\tau$ provides a certain measure of internuclear coupling effects, distilled from unrelated factors. For STIPDOR, generalized SEDOR, $m(t)$ becomes

$$m(t) = \prod_{n=1}^{N} [(1-f) + f\cos(a_n t/2)], \tag{12}$$

where the product is taken over all the ^{63}Cu neighbors of the ^{17}O. f is the probability that a given neighbor is flipped, equal to $\sin^2(\phi/2)$ for the simplest case. In the limit of f (or equivalently ϕ) tends to zero, we can discard terms beyond first order in f to find

$$m(t) \approx [1 - Nf] + f\sum_{n=1}^{N} \cos(a_n t/2). \tag{13}$$

Upon Fourier transform of $m(t)$ the coupling frequencies now appear directly.

Figure 14 shows the ^{17}O-^{63}Cu spin-echo double-resonance (SEDOR) signal for a pulse of independently measured $f = 4.7\%$. Later we shall discuss the fit employed in Fig. 1, but now we only state that the beats observed in Fig. 1 reveal directly the coupling frequency $^{17,63}a$ between nearest-neighbor ^{17}O and ^{63}Cu nuclei in the $YBa_2Cu_3O_7$ planes. Fitting the curve of Fig. 1 to an appropriate functional form yields a coupling strength $(2\pi)^{-1}[^{63,17}a/2]_{tot} = (427 \pm 10)$ Hz. The major part of this coupling is direct nuclear magnetic dipole coupling, which contributes a known amount $(2\pi)^{-1}[^{63,17}a/2]_{dipole} = (2\pi)^{-1}(^{63}\gamma {}^{17}\gamma \hbar / r^3)(1 - 3\cos^2\theta)/2 = 281$ Hz. Thus the remaining amount, (147 ± 10) Hz, is the contribution from "indirect" or electron-mediated coupling.[47]

To summarize, then, we find that the nearest-neighbor ^{63}Cu-^{17}O coupling is given by $(2\pi)^{-1}[^{63,17}a/2] = (147 \pm 10)$ Hz.
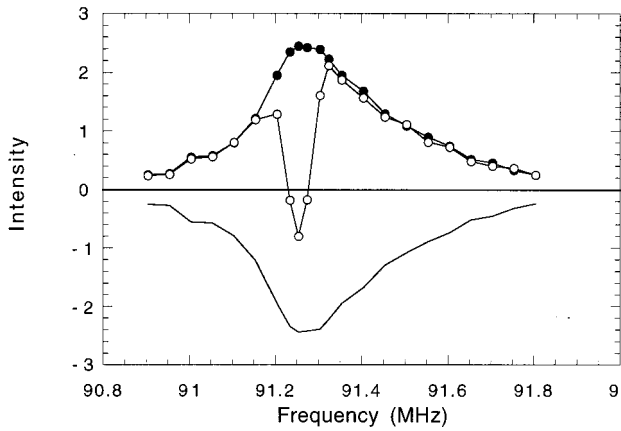
FIG. 15. Closed circles map the $T=5$ K ^{63}Cu(2) line shape. Also shown is the line shape multiplied by -1. Open circles are the measured line shape taken immediately following a ''prepulse,'' which iteself is identical to the ^{63}Cu pulse used in the SEDOR experiment of Fig. 14. Comparison of the mapped line shape with and without the prepulse reveals quantitatively the efficacy of the ^{63}Cu pulse, which we use to analyze the amplitude of the SEDOR signal of Fig. 14.

2. Amplitude of the beats

In accordance with Eq. (2) we fitted the data in Fig. 1 to the functional form $m(t) = [(1-f)+f\cos(^{17,63}at/2)]^2 \exp(-t/\tau_2)$. The first factor is squared to reflect the presence of two identical nearest neighbors, and then the exponential is included to incorporate the effects of all other neighbors. (A true exponential is not realistic, since it has a diverging second moment. However, it provided a somewhat better fit than did the Gaussian form.) The best fit provided the coupling frequency given earlier and a ''flipping'' parameter f of 2.1%. For 100% abundant, spin-$\frac{1}{2}$ nuclei, f should be equal to $\sin^2(\phi/2)$. For spin-$\frac{3}{2}$ ^{63}Cu, which is 69% abundant, however, our pulse is applied only to the $(\frac{1}{2}, -\frac{1}{2})$ transition, with other transitions shifted away by quadrupole splittings. Together these factors give $f = (\frac{1}{2}) \times(.69)\sin^2[\phi_{\rm eff}/2]$. Finally, the Cu line shape in the superconducting state is rather broad and thus it was not possible to cover the entire line shape uniformly. To assess this final complication we ran a separate ^{63}Cu experiment as follows: we first mapped the ^{63}Cu line shape. Then we remapped the line shape, but now with a ''prepulse,'' identical to the ^{63}Cu pulse in the SEDOR experiment, applied immediately before. The results of this experiment are shown in Fig. 15. The ''flipped'' area of Fig. 15 is approximately (13.6 ± 1)% of that which would be obtained in a perfect ''180°'' pulse which would invert the entire line shape. Then we expect $f = (\frac{1}{2})(.69)[0.136] = (4.7\pm0.3)$%, which is more than twice as large as the measured $f = 2.1$%.

Why then, is the amplitude of the beats in Fig. 14 too small by more than a factor of 2? One suggestion is that a substantial fraction of the ^{63}Cu nuclear spins, well more than half, are undergoing rapid mutual spin flips. The issue of mutual spin flips impacts upon a difference in interpretation that has existed in the literature. Recchia *et al.*[45] recently

measured and analyzed the normal-state T_2 behavior of ^{17}O. They inferred that the ^{17}O T_2 behavior was dominated by the ^{17}O-^{63}Cu coupling, modulated in time by the ^{63}Cu Zeeman transitions (T_1 processes). However, their analysis required a phenomenological enhancement of the ^{17}O-^{63}Cu coupling strength to a value some 59% above the dipole coupling value. Confronting similar experimental results, Keren *et al.*[48] and Walstedt[8] proposed instead that rapid ^{63}Cu-^{63}Cu mutual spin flips (flip rate of order $(100~\mu s)^{-1}$ for the case of YBa$_2$Cu$_3$O$_7$) rather than a coupling enhancement, was required. From this Keren *et al.* inferred consequences regarding the magnetic phase diagram classification of YBa$_2$Cu$_3$O$_7$ within the framework of Sokol and Pines.[27]

With one exception our new findings support the picture of Recchia *et al.* and, furthermore, we note that our agreement with their findings for normal state measurements shows that our conclusions here must apply above T_c as well as at the low temperature (4.2 K) of our measurement. We directly measure a ^{63}Cu-^{17}O spin coupling frequency which is enhanced by some (52 ± 4)% above the expected dipole coupling strength, in reasonable agreement with Recchia *et al.*'s inferred enhancement of 59%. The exception of course is that the experimentally obtained f is smaller than expected. This could indicate that some fraction of the ^{63}Cu spins undergo rapid mutual spin flips, because if such flips occur at rates exceeding the ^{63}Cu-^{17}O coupling frequencies, then the effects of ^{63}Cu-^{17}O coupling is ''motionally averaged'' away.[40,49] [Intuitively one can understand that if the ^{63}Cu spins are already undergoing very rapid spin flips, then the act of flipping the ^{63}Cu's once more with an applied rf pulse, as shown for the ''ϕ'' pulse applied to the ''S'' spins in Fig. 1, will have little effect upon the ^{17}O signal (the ''I'' spins of Fig. 1).]

In order to test this hypothesis, that the amplitude f is reduced from the expected value because some fraction of the ^{63}Cu spins undergo rapid mutual spin flips, we again performed a STIPDOR experiment, measuring ^{17}O while flipping ^{63}Cu. However, this time we flipped the ^{63}Cu satellite $(\frac{3}{2}, \frac{1}{2})$ transition. If we assume that a large fraction of the ^{63}Cu nuclei undergo rapid mutual spin flips between $+\frac{1}{2}$ and $-\frac{1}{2}$ (note that rapid flips between $+\frac{3}{2}$ and $+\frac{1}{2}$ or between $-\frac{3}{2}$ and $-\frac{1}{2}$ are not expected, because these transitions have large inhomogeneous broadening which ''detunes'' mutual spin flips), then a ''flip'' from $\frac{3}{2}$ to $\frac{1}{2}$ is effectively a flip of ''$\Delta m = \frac{3}{2}$.'' Then one would expect that the ''beat'' frequency that would be observed in this experiment would be $\frac{3}{2}$ as great as that observed in Fig. 14. Figure 16 shows that this is not the case. It shows the data of Fig. 14 (flipping ^{63}Cu central transition) together with ^{17}C-^{63}Cu in which the ^{63}Cu satellite $(\frac{3}{2}, \frac{1}{2})$ transition is flipped. The beat frequencies observed are identical for these two cases. From this result we can infer that there is *not* a large fraction of ^{63}Cu spins undergoing mutual spin flips.

3. Summary of ^{63}Cu-^{17}O measurements

Figure 14 demonstrates that the nearest-neighbor ^{63}Cu-^{17}O electron mediated nuclear spin-spin coupling $^{63,17}a$ is given by $(2\pi)^{-1}[^{63,17}a/2] = (147\pm10)$ Hz. Though the
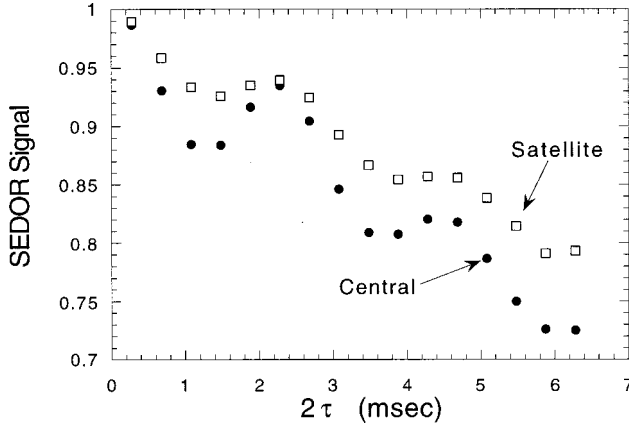
FIG. 16. Closed circles is the SEDOR signal of Fig. 14. Open circles is the same SEDOR experiment, except that the ^{63}Cu pulse is applied to the ^{63}Cu satellite $(\frac{3}{2}, \frac{1}{2})$ transition rather than the central $(\frac{1}{2}, -\frac{1}{2})$. The identical beat frequencies observed demonstrates that most of the ^{63}Cu spins within the central transition are not undergoing rapid mutual spin flips.

amplitude of the beats observed in the experiment is smaller than expected, there is direct evidence (Fig. 16) that few if any ^{63}Cu's undergo rapid mutual spin flips.

IV. IMPLICATIONS FOR THEORY

The experimental results of Sec. III impact broadly upon the previous analyses of NMR data, and hence they also should affect the picture of the normal-state electronic structure of the high-T_c cuprates. We shall show below that the ''one-component model,'' in which one tries to fit all NMR data using a single spin degree of freedom per Cu atom, is not sufficiently rich.

The connection between electronic spin susceptibility $\chi'(\mathbf{q},\omega)$ and nuclear-spin coupling between ^{17}O at site I and ^{63}Cu at site j is given by $^{17,63}a_{i,j}$[25,36,50]

$$^{17,63}a_{i,j}=[2\mu_B]^{-2}\sum_l \sum_k {}^{17}A(i,k)\chi'$$

$$\times (\mathbf{r}_l-\mathbf{r}_k,\omega=0)^{63}A(j,l). \quad (14)$$

Here $^{17}A(i,k)$ is the hyperfine coupling of the ^{17}O nuclear species at site i to the electron spin at Cu site k, and $\chi'(\mathbf{r}_l -\mathbf{r}_k,\omega=0)$ is the electron spin response at site 1 to a delta function magnetic field applied at site k. The analogous formula for ^{63}Cu-^{63}Cu couplings $^{63,63}a$ is

$$^{63,63}a_{i,j}=[2\mu_B]^{-2}\sum_l \sum_k {}^{63}A(i,k)\chi'$$

$$\times (\mathbf{r}_l-\mathbf{r}_k,\omega=0)^{63}A(j,l). \quad (15)$$

We stress the simplicity of these formulas—spin-spin couplings measure a static spin response to a known, localized applied effective magnetic field.

It is beyond the scope of this paper to provide a full review of the application of ''one-component'' theories to NMR data. However, it suffices to say that the parameters needed to calculate $^{63,63}a$ and $^{63,17}a$ from Eqs. (14) and (15) are tightly constrained from past experiment.[3,5,6,13] Millis, Monien, and Pines provided a phenomenological form:

$$\chi'(\mathbf{q},\omega=0)\propto[1+(\mathbf{q}-\mathbf{Q})^2\xi^2]^{-1} \quad (16)$$

for the spin susceptibility, characterized by a antiferromagnetic correlations with length scale ξ. This form was updated by Zha, Barzhykin, and Pines[13] to include incommensuration. A key requirement is that the correlation length ξ must be at least two to three lattice constants, if the model is to explain the sharply contrasting behaviors of $^{63}(T_1T)^{-1}$ and $^{17}(T_1T)^{-1}$.

The magnitudes and spatial dependences of the hyperfine couplings $^{17}A(i,k)$ and $^{63}A(j,l)$ are well established.[4–6,51,52] ^{63}Cu has a coupling A_c to the onsite electron spin and a transferred coupling B to the four nearest Cu neighbors. We use ^{17}O hyperfine coupling to the two nearest-neighbor Cu's only, with magnitude C_c. From both *a priori* and experimental considerations one finds that $A_c\approx-4B$ $\approx-1.69\times10^{-6}$ eV (Refs. 4, 5, 51, and 53) and C_c $\approx0.24\times10^{-6}$ eV.[6,54]

We first remark briefly the ^{63}Cu-^{63}Cu coupling. As we discussed in Ref. 34, existing measurements of T_{2G} provide a constraint, namely the sum of the squares of the couplings between a single ^{63}Cu and all of its ^{63}Cu neighbors. In that work we noted that the nearest-neighbor coupling alone, $(2\pi)^{-1}[^{63,63}a/2]=(900\pm100)$ Hz, was almost enough to account for the entire T_{2G} decay, leaving little room for couplings to extend out to several lattice constants. Yet the large correlation length ξ needed to explain $^{63}(T_1T)^{-1}$ and $^{17}(T_1T)^{-1}$ would necessarily imply nuclear spin couplings to extend out several lattice constants. We have learned[50,55] though that these ^{63}Cu-^{63}Cu coupling measurements can be explained quantitatively with a reasonably large value of ξ if one includes incommensuration of 20–25%, which is itself observed experimentally.[56–58] It is not clear though that these parameters can still be used to understand $^{63}(T_1T)^{-1}$ and $^{17}(T_1T)^{-1}$.

The combination, though, of $^{63,17}a$ and $^{63,63}a$ provides yet more problems for the one-component model. The issue is that the cancellation effects which supposedly result in the very different behaviors of $^{63}(T_1T)^{-1}$ and $^{17}(T_1T)^{-1}$ should also be present in comparison of $^{63,17}a$ and $^{63,63}a$. The ratio $(^{63,17}a/^{63,63}a)$ is given from Eqs. (14) and (15) as

$$^{17,63}a/^{63,63}a=\frac{(AC+BC)\chi'_{0,0}+(AC+4BC)\chi'_{1,0}+(2BC)\chi'_{1,1}+BC\chi'_{2,0}}{2AB\chi'_{0,0}+(A^2+9B^2)\chi'_{1,0}+4AB\chi'_{1,1}+2AB\chi'_{2,0}+6B^2\chi'_{2,1}+B^2\chi'_{3,0}}. \quad (17)$$
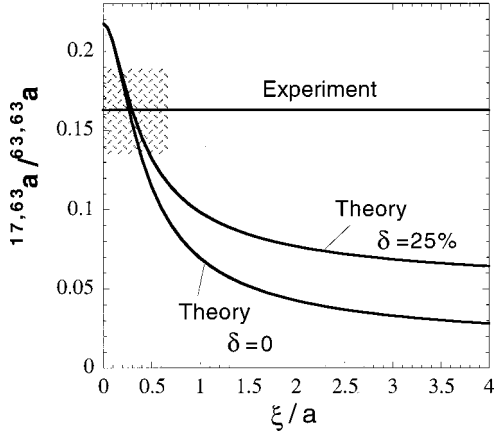
FIG. 17. Theoretical prediction of the ratio $^{17,63}a/^{63,63}a$ vs electron-spin correlation length ξ, in units of lattice constant a, according to Eqs. (16) and (17), and the experimentally measured value. Theoretical curves are shown for $\delta=0$ (antiferromagnetic correlations) and $\delta=25\%$ (incommensurate correlations). Uncertainty in the experimental and theoretical curves are each $\sim15\%$. Uncertainty in the theoretical curves results from uncertainty of hyperfine coupling parameters. The shaded region of overlap between theory and experiment indicates a correlation length less than 0.6.

In this notation $\chi'_{i,j}$ is the real space response of the spin system at lattice position (i,j) to a unit of magnetic-field strength applied at the origin. For the case of no electron-spin correlations Eq. (17) reduces to $^{17,63}a/^{63,63}a=(AC+BC)/(2AB)=0.22\pm0.03$, as compared with the experimental value of 0.16 ± 0.02. To parametrize more general possibilities for χ' we use the Millis-Monien-Pines (MMP) expression,[5] generalized by Zha-Barzykin-Pines (ZBP) (Ref. 13) to allow for incommensuration:

$$\chi'(\mathbf{q})\propto\sum_j \left[1+|\mathbf{q}-\mathbf{Q}_j|^2\xi^2\right]^{-1}, \qquad (18)$$

where the four $\mathbf{Q}_j$ values are $\mathbf{Q}_j=[\pi(1\pm\delta),\pi(1\pm\delta)]$. The parameter δ is zero for the case of antiferromagnetic correlations, as in the original MMP formulation, but in ZBP it characterizes the incommensuration of the correlations, and is taken to be as large as 25%.

Figure 17 shows the predicted ratio $^{17,63}a/^{63,63}a$ from Eqs. (3) and (4), along with $^{17,63}a/^{63,63}a$ from experiment, plotted vs correlation length ξ. Theoretical curves are shown for both $\delta=0$ (antiferromagnetic correlations) and $\delta=.25$ (incommensurate correlations). The region of overlap of theory and experiment (with associated uncertainties of each) specifies that the correlation length ξ must be *less than 0.6 lattice constants*, much less than the value of two to three lattice constants needed to explain the sharp contrasts in ^{17}O and ^{63}Cu spin-lattice relaxation behaviors. The clear physical interpretation is that the expected spin correlations would result in cancellation, or ''form-factor'' effects, that would reduce $^{17,63}a$ relative to $^{63,63}a$. The unexpectedly large experimental value of $^{17,63}a/^{63,63}a$ tells us that the spin correlations are not present.
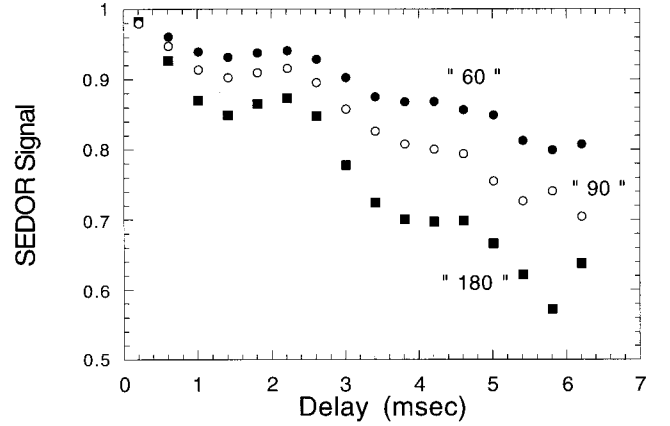

FIG. 18. The ^{63}Cu-^{17}O double resonance STIPDOR measurements of Fig. 14 are repeated here on a sample of oxygen reduced YBa$_2$Cu$_3$O$_{6+x}$, with T_c of ~60 K. The beat frequency observed there, for the $T_c=60$-K sample, is approximately the same as that observed in $T_c\sim90$-K material. Yet in the $T_c=60$-K materials it is much more clearly established through inelastic neutron scattering that electron-spin correlation lengths are at least several lattice constants.

There are disturbing aspects to the conclusion drawn above, and we stress that we do *not* conclude that the electron-spin correlation length is less than one. First, the very short correlation length inferred makes it impossible to explain the contrasting temperature dependences of ^{17}O and ^{63}Cu spin lattice relaxation rates in terms of the commonly invoked picture[5-7] involving antiferromagnetic fluctuations and hyperfine cancellation effects at the ^{17}O. A related problem is that if one takes the limit of $\xi=0$, then the measured coupling $^{17,63}a$ is given by $^{17,63}a=(A_c+B)\chi'_{0,0}C_c$, and from this one can infer that $(\chi'_{0,0}/\mu_B^2)\approx16$ states/(eV Cu). $\chi'_{0,0}$ is the average over the first Brillouin zone of $\chi'(\mathbf{q})$, but Knight shift measurements[5,6,53] indicate that $[\chi'(\mathbf{q}=0)/\mu_B^2]\approx2.5-3$ states/(eV Cu) or six times smaller than the required $\mathbf{q}$ space average, $\chi'_{0,0}$. Thus there must be some peaking in $\mathbf{q}$ space away from $\mathbf{q}=0$, but it can not be too sharp. It appears though that it is not possible to find a set of values of $\chi'(\mathbf{q}=0)$ and ξ that can explain the Knight shift and spin-spin coupling consistently.

We have also repeated the ^{63}Cu-^{17}O measurements of Fig. 14 on a sample of oxygen reduced YBa$_2$Cu$_3$O$_{6+x}$, with T_c of ~60-K. The results are shown in Fig. 18. The beat frequency observed there, for the $T_c=60$-K sample is approximately the same as that observed in $T_c\sim90$-K material. Yet in the $T_c=60$-K materials it is much more clearly established through inelastic neutron scattering that electron spin correlation lengths are at least several lattice constants.

Therefore again we do *not* conclude from Fig. 14 that the electron-spin correlation length ξ is small, less than one; we conclude, rather, that the application of the one-component model to the full body of high-T_c NMR data does not yield any self-consistent understanding.

What assumptions are present in this one-component model, and which assumptions could be misguided? NMR Knight shift and T_1 parameters can be calculated directly

from the $\mathbf{q}$ and ω-dependent electron-spin susceptibility $\chi(\mathbf{q},\omega)$.[1-3] Within the one-component model it is assumed that the $\mathbf{r}$-dependent electron-spin susceptibility need only be specified on the Cu atomic sites, and not defined on a finer length scale. In terms of reciprocal space, this means that $\chi(\mathbf{q},\omega)$ must be defined only over the first Brillouin zone. If the full array of NMR experiment cannot be explained using a consistent set of hyperfine coupling parameters and the same $\chi(\mathbf{q},\omega)$, then there is an indication that the one-component model is not adequate. One might suspect that electron dynamics on the oxygen sites have behavior which is more independent from that of the Cu than previously believed. A second possibility is that effects of stripes, which have become increasingly clear in oxygen reduced T_c $=60$-K material,[57] may also be present in $T_c=90$-K $YBa_2Cu_3O_7$, and that these effects could explain some or all of the observations. More generally the possibility of spatial inhomogeneities[59] in the charge and spin properties would require reanalysis of our data. The smaller than expected amplitude of the beats observed in Fig. 14 (and discussed above) might indicate that only a subset of the ^{17}O spins see the anomalously strong ^{63}Cu-^{17}O coupling strength observed there. These, however, are not yet well defined speculations.

[1] C. Berthier, M. H. Julien, M. Horvatic, and Y. Berthier, J. Phys. I **6**, 2205 (1996).

[2] C. H. Pennington and C. P. Slichter, in *Physical Properties of High Temperature Superconductors*, edited by D. M. Ginsberg (World Scientific, Singapore, 1990), Vol. 2, p. 269.

[3] C. P. Slichter, in *Strongly Correlated Electronic Materials*, edited by Z. W. K. S. Bedell, D. E. Meltzer, A. V. Balatsky, and E. Abrahams (Addison-Wesley, Reading, MA, 1993), p. 427.

[4] F. Mila and T. M. Rice, Physica C **157**, 561 (1989).

[5] A. J. Millis, H. Monien, and D. Pines, Phys. Rev. B **42**, 167 (1990).

[6] H. Monien, D. Pines, and M. Takigawa, Phys. Rev. B **43**, 258 (1991).

[7] B. Shastry, Phys. Rev. Lett. **63**, 1288 (1989).

[8] R. E. Walstedt and S.-W. Cheong, Phys. Rev. B **51**, 3163 (1995).

[9] R. E. Walstedt and S.-W. Cheong, Phys. Rev. B **53**, R6030 (1996).

[10] R. E. Walstedt, B. S. Shastry, and S.-W. Cheong, Phys. Rev. Lett. **72**, 3610 (1994).

[11] M. Horvatic, C. Berthier, Y. Berthier, and P. Segransan, Phys. Rev. B **48**, 13 848 (1993).

[12] J. A. Martindale, P. C. Hammel, W. L. Hults, and J. L. Smith, Phys. Rev. B **57**, 11 769 (1998).

[13] Y. Zha, V. Barzykin, and D. Pines, Phys. Rev. B **54**, 7561 (1996).

[14] V. A. Nandor, J. A. Martindale, O. M. Vyaselev, C. H. Pennington, L. Hults, and J. L. Smith, Phys. Rev. B **60**, 6907 (1999).

[15] M. Takigawa, W. L. Hults, and J. L. Smith, Phys. Rev. Lett. **71**, 2650 (1993).

[16] V. Barzykin and D. Pines, Phys. Rev. B **52**, 13 585 (1995).

[17] N. Bulut and D. J. Scalapino, Phys. Rev. Lett. **67**, 2898 (1991).

[18] N. Bulut and D. J. Scalapino, Physica C **185-189**, 1581 (1991).

[19] N. J. Curro, T. Imai, C. P. Slichter, and B. Dabrowski, Phys. Rev. B **56**, 877 (1997).

[20] T. Imai, C. P. Slichter, A. P. Paulikas, and B. Veal, Phys. Rev. B **47**, 9158 (1993).

[21] T. Imai, C. P. Slichter, K. Yoshimura, and M. Katoh, Phys. Rev. Lett. **71**, 1254 (1993).

[22] Y. Itoh, H. Yasuoka, Y. Fujiwara, Y. Ueda, T. Machi, I. Tomeno, K. Tai, N. Koshizuka, and S. Tanaka, J. Phys. Soc. Jpn. **61**, 1287 (1992).

[23] Y. Itoh, H. Yasuoka, and Y. Ueda, J. Phys. Soc. Jpn. **59**, 3463 (1990).

[24] C. H. Pennington, D. J. Durand, C. P. Slichter, J. P. Rice, E. D. Bukowski, and D. M. Ginsberg, Phys. Rev. B **39**, 274 (1989).

[25] C. H. Pennington and C. P. Slichter, Phys. Rev. Lett. **66**, 381 (1991).

[26] C. P. Slichter, R. L. Corey, N. J. Curro, S. M. DeSoto, K. O'Hara, T. Imai, A. M. Kini, H. H. Wang, U. Geiser, J. M. Williams, K. Yoshimura, M. Katoh, and K. Kosuge, Philos. Mag. B **74**, 545 (1996).

[27] A. Sokol and D. Pines, Phys. Rev. Lett. **71**, 2813 (1993).

[28] R. Stern, M. Mali, J. Roos, and D. Brinkmann, Phys. Rev. B **51**, 15 478 (1995).

[29] M. Takigawa, Phys. Rev. B **49**, 4158 (1994).

[30] M. Takigawa, N. Motoyama, H. Eisaki, and S. Uchida, Phys. Rev. Lett. **76**, 4612 (1996).

[31] M. Takigawa, O. A. Starykh, A. W. Sandvik, and R. R. P. Singh, Phys. Rev. B **56**, 13 681 (1997).

[32] D. Thelen and D. Pines, Phys. Rev. B **49**, 3528 (1994).

[33] D. Thelen, D. Pines, and J. P. Lu, Phys. Rev. B **47**, 9151 (1993).

[34] K. R. Gorny, O. M. Vyaselev, S. Yu, C. H. Pennington, W. L. Hults, and J. L. Smith, Phys. Rev. Lett. **81**, 2340 (1998).

[35] T. Gullion and C. Pennington, Chem. Phys. Lett. **290**, 88 (1998).

[36] S. Yu, K. R. Gorny, J. A. Martindale, C. H. Pennington, W. L. Hults, and J. L. Smith, Phys. Rev. Lett. **83**, 3924 (1999).

[37] H. S. Gutowsky, D. W. McCall, and C. P. Slichter, J. Chem. Phys. **21**, 279 (1953).

[38] E. L. Hahn and D. E. Maxwell, Phys. Rev. **88**, 1070 (1952).

[39] R. R. Ernst, G. Bodenhausen, and A. Wokaun, *Principles of Nuclear Magnetic Resonance in One and Two Dimensions* (Clarendon, Oxford, 1987).

[40] C. P. Slichter, *Principles of Magnetic Resonance* (Springer, New York, 1996).

[41] B. Herzog and E. L. Hahn, Phys. Rev. **103**, 148 (1956).

[42] D. E. Kaplan and E. L. Hahn, J. Phys. Radium **19**, 821 (1958).

[43] T. Gullion, J. Magn. Reson., Ser. A **139**, 402 (1999).

[44] T. S. Cull, J. M. Joers, and T. Gullion, J. Magn. Reson., Ser. A **133**, 352 (1998).

[45] C. H. Recchia, J. A. Martindale, C. H. Pennington, W. L. Hults, and J. L. Smith, Phys. Rev. Lett. **78**, 3543 (1997).

[46] J. A. Martindale, S. E. Barrett, D. J. Durand, K. E. Ohara, C. P. Slichter, W. C. Lee, and D. M. Ginsberg, Phys. Rev. B **50**, 13 645 (1994).

[47] Here we have assumed that the dipolar and indirect couplings add constructively, rather than destructively. As we show in Sec. IV, one may calculate the indirect coupling from known hyperfine couplings and a known electron-spin susceptibility. Using typical values that are proposed one expects that our assumption will be correct. If our assumption is not correct, then we would need to infer an indirect coupling of $(281+427)$ Hz$=708$ Hz, rather than 147 Hz. 147 Hz is already anomalously large, as we shall see, and therefore we do not consider the alternate possibility, that the coupling is even larger and of unexpected sign.

[48] A. Keren, H. Alloul, P. Mendels, and Y. Yoshinari, Phys. Rev. Lett. **78**, 3547 (1997).

[49] A. Abragam, *The Principles of Nuclear Magnetism* (Clarendon, Oxford, 1961).

[50] J. Haase, D. K. Morr, and C. P. Slichter, Phys. Rev. B **59**, 7191 (1999).

[51] A. Abragam and B. Bleaney, *Electron Paramagnetic Resonance of Transition Ions* (Dover, New York, 1970).

[52] C. H. Pennington, D. J. Durand, C. P. Slichter, J. P. Rice, E. D. Bukowski, and D. M. Ginsberg, Phys. Rev. B **39**, 2902 (1989).

[53] S. E. Barrett, D. J. Durand, C. H. Pennington, C. P. Slichter, T. A. Friedmann, J. P. Rice, and D. M. Ginsberg, Phys. Rev. B **41**, 6283 (1990).

[54] Y. Yoshinari, Ph.D. thesis, Institute for Solid State Physics, Tokyo University, Tokyo, 1992.

[55] D. Morr (private communication).

[56] H. Mook, P. Dai, R. D. Hunt, and F. Dogan, cond-mat/9712326.

[57] H. A. Mook, P. C. Dai, F. Dogan, and R. D. Hunt, Nature (London) **404**, 729 (2000).

[58] H. A. Mook, M. Yethiraj, G. Aeppli, T. E. Mason, and T. Armstrong, Phys. Rev. Lett. **70**, 3490 (1993).

[59] D. K. Morr, J. Schmalian, and D. Pines, cond-mat/0002164.